Available online at www.sciencedirect.com
ScienceDirect
Biochimie 89 (2007) 135–144
BIOCHIMIE
www.elsevier.com/locate/biochi

Inhibition of plant amine oxidases by a novel series of diamine derivatives

Jana Stránská [a], Marek Šebela [a,*], Petr Tarkowski [a], Pavel Řehulka [b], Josef Chmelík [b], Igor Popa [c], Pavel Peč [a]

[a] *Department of Biochemistry, Faculty of Science, Palacký University, Šlechtitelů 11, 783 71 Olomouc, Czech Republic*
[b] *Institute of Analytical Chemistry, Czech Academy of Sciences, Veveří 97, 611 42 Brno, Czech Republic*
[c] *Laboratory of Growth Regulators, Palacký University and Institute of Experimental Botany – Czech Academy of Sciences, Šlechtitelů 11, 783 71 Olomouc, Czech Republic*

Received 5 May 2006; accepted 16 August 2006
Available online 11 September 2006

Abstract

A series of *N*,*N*′-bis(2-pyridinylmethyl)diamines was synthesized and characterized for their inhibition effects towards plant copper-containing amine oxidase (EC 1.4.3.6) and polyamine oxidase (EC 1.5.3.11), which mediate the catabolic regulation of cellular polyamines. Even though these enzymes catalyze related reactions and, among others, act upon two common substrates (spermidine and spermine), their molecular and kinetic properties are different. They also show a different spectrum of inhibitors. It is therefore of interest to look for compounds providing a dual inhibition (i.e. inhibiting both enzymes with the same inhibition potency), which would be useful in physiological studies involving modulations of polyamine catabolism. The synthesized diamine derivatives comprised from two to eight carbon atoms in the alkyl spacer chain. Kinetic measurements with pea (*Pisum sativum*) diamine oxidase and oat (*Avena sativa*) polyamine oxidase demonstrated reversible binding of the compounds at the active sites of the enzymes as they were almost exclusively competitive inhibitors with K_i values ranging from 10^{-5} to 10^{-3} M. In case of oat polyamine oxidase, the K_i values were significantly influenced by the number of methylene groups in the inhibitor molecule. The measured inhibition data are discussed with respect to enzyme structure. For that reason, the oat enzyme was analyzed by de novo peptide sequencing using mass spectrometry and shown to be homologous to polyamine oxidases from barley (isoform 1) and maize. We conclude that some of the studied *N*,*N*′-bis(2-pyridinylmethyl)diamines might have a potential to be starting structures in design of metabolic modulators targeted to both types of amine oxidases.

Keywords: Active site; Diamine oxidase; Inhibition; *N*,*N*′-bis(2-pyridinylmethyl)diamine; Polyamine oxidase

1. Introduction

Polyamines (i.e. putrescine, spermidine and spermine) are ubiquitous cationic compounds, which are involved in crucial physiological events including cell growth and differentiation [1]. Polyamine levels are maintained through biosynthetic and biodegradation pathways or by transport [1,2]. Ornithine decarboxylase (EC 4.1.1.17), spermidine synthase (EC 2.5.1.16) and spermine synthase (EC 2.5.1.22) have been recognized as key biosynthetic enzymes for polyamines [1]. The oxidative degradation of polyamines is catalyzed by quinoprotein copper-containing amine oxidases (CAOs, EC 1.4.3.6)

Abbreviations: BPAO, barley polyamine oxidase; BPBD, N^1,N^4-bis(2-pyridinylmethyl)-1,4-butanediamine; BPED, N^1,N^2-bis(2-pyridinylmethyl)-1,2-ethanediamine; BPHD, N^1,N^7-bis(2-pyridinylmethyl)-1,7-heptanediamine; BPOD, N^1,N^8-bis(2-pyridinylmethyl)-1,8-octanediamine; BPPD, N^1,N^5-bis(2-pyridinylmethyl)-1,5-pentanediamine; BPRD, N^1,N^3-bis(2-pyridinylmethyl)-1,3-propanediamine; BPXD, N^1,N^6-bis(2-pyridinylmethyl)-1,6-hexanediamine; CAO, copper-containing amine oxidase; CHCA, α-cyano-4-hydroxycinnamic acid; ESI, electrospray ionization; MPAO, maize polyamine oxidase; MALDI, matrix-assisted laser desorption/ionization; MS, mass spectrometry; MS/MS, tandem mass spectrometry; OPAO, oat polyamine oxidase; PAO, polyamine oxidase; PSAO, pea seedling amine oxidase; Put, putrescine; Spd, spermidine; TOF, time of flight.

* Corresponding author. Tel.: +420 585634927; fax: +420 585634933.
E-mail address: marek.sebela@upol.cz (M. Šebela).

0300-9084/$ - see front matter © 2006 Elsevier Masson SAS. All rights reserved.
doi:10.1016/j.biochi.2006.08.001

and flavoprotein polyamine oxidases (PAOs, EC 1.5.3.11) [2]. As it is considered in the classification of the enzymes, CAOs attack primary amino groups of substrates, whereas PAOs attack secondary amino groups. CAOs are usually homodimers comprising an active site with topaquinone cofactor and a cupric ion in each of the subunits [2]. In plants, CAOs preferentially oxidize diamines like putrescine or cadaverine and for that reason they are often called diamine oxidases [3]. The oxidative deamination of CAO substrates results in the corresponding aldehydes, ammonium ions and hydrogen peroxide. PAOs are monomeric proteins containing a non-covalently bound FAD cofactor [2]. They catalyze the oxidative cleavage of spermine and spermidine at their secondary amino groups. Plant PAOs produce 4-aminobutanal (from spermidine) or *N*-(3-aminopropyl)-4-aminobutanal (from spermine), hydrogen peroxide and 1,3-propanediamine [2]. Molecular and kinetic properties of plant CAOs and PAOs have been recently reviewed [4,5]. Representative members of the enzymes were crystallized and thoroughly characterized with respect to structure–functional relationships [6,7].

Inhibitors represent important tools in the study of catalytic properties of enzymes and they also find a broad application in physiological research. Both CAOs and PAOs show their own spectrum of inhibitors, which reflect the architecture and composition of the active sites [5,8,9]. In case of pea seedling enzyme as a representative of plant CAOs, the active site of each subunit lies near an edge of the largest β-sandwich domain, but is not accessible from the solvent [6]. The essential active site copper atom is coordinated by three histidine side chains and two water molecules in an approximately square–pyramidal arrangement [6]. The active site of maize PAO (MPAO) consists of a long U-shaped catalytic tunnel, whose innermost part is located in front of the flavin ring [7]. Plant CAOs are inhibited by substrate analogs (diamines, diaminoketones), hydrazines (producing irreversible inactivation), copper-complexing agents and some alkaloids [8]. Typical inhibitors of plant PAOs are long-chain amine compounds guazatine, MDL72527 and other polyamine analogs (e.g. C8, C10 and C12 diamines). They are also inhibited by acridine dyes and hydrazine derivatives [5,9].

In most cases, plant CAO and PAO inhibitors show a divergence with respect to chemical structure and/or inhibition effect to each individual enzyme. It is therefore of interest to look for inhibitors providing a dual inhibition i.e. inhibiting both CAOs and PAOs with the same inhibition potency. We synthesized a series of homologous *N*,*N*′-bis(2-pyridinylmethyl)diamines comprising from two to eight carbon atoms in the diamine spacer chain. The dumbbell-shaped structure was chosen for two reasons: it resembles polyamines in length and positioning of nitrogen atoms and the pyridine rings may facilitate hydrophobic binding at the active site. Additionally, in the case of CAOs, one could expect possible ligand properties of the pyridine nitrogen atoms towards the enzyme's copper. Indeed, kinetic measurements with pea diamine oxidase (PSAO) and oat polyamine oxidase (OPAO) demonstrated that the synthesized compounds were inhibitors of both enzymes. The latter enzyme was purified by a new method and analyzed for structural informations by MALDI-TOF MS and MS/MS to discuss the inhibition results. The measured K_i values were in the range 10^{-5}–10^{-3} M. Several of the compounds showed the same inhibition mode and potency for both PSAO and OPAO.

2. Materials and methods

2.1. Chemicals

2-Pyridinecarboxaldehyde was from Acros (Geel, Belgium), DEAE-cellulose (Cat. no. D6418) and sodium borohydride were from Sigma–Aldrich Chemie (Steinheim, Germany). 1,2-Ethanediamine; 1,3-propanediamine; putrescine (1,4-butanediamine); cadaverine (1,5-pentanediamine); 1,6-hexanediamine; 1,7-heptanediamine; 1,8-octanediamine and spermidine trihydrochloride were purchased from Sigma–Aldrich Chemie. A hydrogen chloride solution in isopropanol was provided by Dr. Zatloukal, Laboratory of Growth Regulators, Faculty of Science, Palacký University. All other chemicals were of analytical purity grade supplied by local distributors.

2.2. Organic syntheses and analyses of the synthesized compounds

The synthesis of homologous *N*,*N*′-bis(2-pyridinylmethyl)-diamines (Fig. 1) utilized a route adapted from the literature [10–12]. 2-Pyridinecarboxaldehyde (52.5 mmol) was added to a solution of C2–C8 diamine in methanol (25 mmol in 25 ml) and the mixture was heated under reflux for 3 h. After cooling to 25 °C, $NaBH_4$ (70 mmol) was added in small portions and the mixture was stirred for 16 h. The reaction was quenched by careful addition of 4 M HCl until a strongly acidic pH was reached and the mixture was stirred for an additional 30 min. Then the solution was made basic using ammonia (12.5% in water), extracted with CH_2Cl_2 (3×50 ml) and the combined organic layers were dried (Na_2SO_4). The product base was obtained as a yellow oil (>70% yield) after evaporation of the solvent under reduced pressure. Then it was converted to a crystalline tetrahydrochloride by adding an excess of hydrogen chloride in isopropanol and recovered by filtration. Recrystallization of the product was achieved by dissolving in hot ethanol, filtration with charcoal, cooling on ice and adding of an excess of ice-cold diethylether. Absorption spectra of water solutions showed a maximum at 260 nm revealing the presence of pyridine moiety. ^{1}H NMR and ^{13}C NMR measurements were performed at 25 °C on

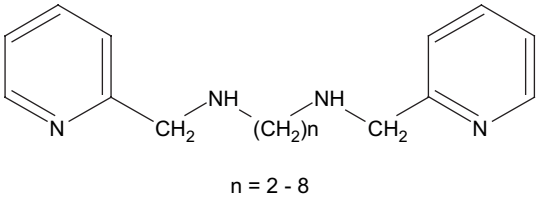

Fig. 1. Chemical structures of the studied inhibitors of plant amine oxidases.

a Bruker AVANCE 300 NMR spectrometer (Bruker BioSpin, Rheinstetten, Germany), operating at a magnetic field strength of 7.05 T. Deuterated dimethylsulfoxide (99.96%) from Sigma–Aldrich Chemie was used as a solvent. Mass spectra were acquired using a Quattro Micro™ triple-stage quadrupole mass spectrometer (Micromass, Manchester, UK) equipped with an electrospray ion source. Positive ionization mode was used producing protonated quasimolecular ions ($[M+H]^+$). All samples were directly introduced to the mass spectrometer by a syringe (flow rate of 10 μl min^{-1}). Parameters of the electrospray were as follows: capillary voltage 3.0 kV, cone voltage 30.0 V, desolvation gas flow 550 L h^{-1}, desolvation temperature 350 °C, source temperature 100 °C. Full scan spectra were obtained by scanning mass range 50–400 amu (0.7 s per scan). Tandem mass spectra (daughter ion scan mode) were obtained by scanning mass range from 50 to *m/z* of appropriate parent ion. Collision cell pressure was kept between 3.0 and 3.5 mbar with argon gas and collision cell energy was 25 eV.

The following characteristics of the synthesized compounds were obtained (measured with the tetrahydrochlorides):

N^1,N^2-Bis(2-pyridinylmethyl)-1,2-ethanediamine (BPED): ^{1}H NMR (300 MHz); δ (ppm): 3.55 (s, 4H, 2 × CH_2), 4.53 (s, 4H, 2 × CH_2), 7.68 (m, 2H, Py), 7.95 (d, $J = 7.9$ Hz, 2H, Py), 8.20 (m, 2H, Py), 8.76 (dd, $J_a = 5.1$ Hz, 2H, Py). ^{13}C NMR (75 MHz); δ (ppm): 42.8 (2 × CH_2), 48.7 (2 × CH_2), 125.1 (CH–Py), 125.2 (CH–Py), 140.8 (CH–Py), 146.4 (CH–Py), 149.6 (C–Py). ESI-MS: *m/z* 243 ($[M+H]^+$); MS/MS, *m/z* (relative intensity): 92 (100) − C_6H_6N, 107 (13) − $C_6H_7N_2$, 118 (10) − $C_7H_6N_2$, 135 (46) − $C_8H_{11}N_2$.

N^1,N^3-Bis(2-pyridinylmethyl)-1,3-propanediamine (BPRD): ^{1}H NMR (300 MHz); δ (ppm): 2.25 (qui, $J = 7.5$ Hz, 2H, CH_2), 3.15 (t, $J = 7.5$ Hz, 4H, 2 × CH_2), 4.48 (s, 4H, 2 × CH_2), 7.76 (m, 2H, Py), 8.09 (d, $J = 7.9$ Hz, 2H, Py), 8.28 (m, 2H, Py), 8.80 (dd, $J_a = 5.3$ Hz, 2H, Py). ^{13}C NMR (75 MHz); δ (ppm): 22.1 (CH_2), 44.2 (2 × CH_2), 48.1 (2 × CH_2), 125.4 (CH–Py), 126.1 (CH–Py), 141.8 (CH–Py), 145.4 (CH–Py), 149.2 (C–Py). ESI-MS: *m/z* 257 ($[M+H]^+$); MS/MS, *m/z* (relative intensity): 70 (18) − $C_3H_6N_2$, 80 (5) − C_5H_6N, 92 (28) − C_6H_6N, 93 (10) − C_6H_7N, 121 (100) − $C_7H_9N_2$, 149 (19) − $C_9H_{13}N_2$.

N^1,N^4-Bis(2-pyridinylmethyl)-1,4-butanediamine (BPBD): ^{1}H NMR (300 MHz); δ (ppm): 1.81 (t, $J = 7.5$ Hz, 4H, 2 × CH_2), 3.02 (t, $J = 7.5$ Hz, 4H, 2 × CH_2), 4.48 (s, 4H, 2 × CH_2), 7.80 (m, 2H, Py), 8.11 (d, $J = 7.9$ Hz, 2H, Py), 8.32 (m, 2H, Py), 8.82 (dd, $J_a = 5.3$ Hz, 2H, Py). ^{13}C NMR (75 MHz); δ (ppm): 22.5 (2 × CH_2), 46.3 (2 × CH_2), 47.9 (2 × CH_2), 125.7 (CH–Py), 126.3 (CH–Py), 142.3 (CH–Py), 145.2 (CH–Py), 149.0 (C–Py). ESI-MS: *m/z* 271 ($[M+H]^+$); MS/MS, *m/z* (relative intensity): 84 (13) − $C_5H_{10}N$, 161 (11) − $C_{10}H_{13}N_2$, 163 (100) − $C_{10}H_{15}N_2$.

N^1,N^5-Bis(2-pyridinylmethyl)-1,5-pentanediamine (BPPD): ^{1}H NMR (300 MHz); δ (ppm): 1.36 (qui, $J = 7.7$ Hz, 2H, CH_2), 1.73 (qui, $J = 7.7$ Hz, 4H, 2 × CH_2), 2.91 (t, $J = 7.7$ Hz, 4H, 2 × CH_2), 4.26 (s, 4H, 2 × CH_2), 7.41 (m, 2H, Py), 7.64 (d, $J = 7.7$ Hz, 2H, Py), 7.87 (m, 2H, Py), 8.61 (d, $J = 4.8$ Hz, 2H, Py). ^{13}C NMR (75 MHz); δ (ppm): 23.1 (CH_2), 24.7 (2 × CH_2), 46.4 (2 × CH_2), 50.4 (2 × CH_2), 123.5 (CH–Py), 123.6 (CH–Py), 137.2 (CH–Py), 149.1 (CH–Py), 152.2 (C–Py). ESI-MS: *m/z* 285 ($[M+H]^+$); MS/MS, *m/z* (relative intensity): 98 (17) − $C_5H_{10}N_2$, 175 (15) − $C_{11}H_{15}N_2$, 177 (100) − $C_{11}H_{17}N_2$.

N^1,N^6-Bis(2-pyridinylmethyl)-1,6-hexanediamine (BPXD): ^{1}H NMR (300 MHz); δ (ppm): 1.33 (qui, $J = 3.8$ Hz, 4H, 2 × CH_2), 1.70 (qui, $J = 7.7$ Hz, 4H, 2 × CH_2), 2.93 (t, $J = 7.7$ Hz, 4H, 2 × CH_2), 4.28 (s, 4H, 2 × CH_2), 7.43 (m, 2H, Py), 7.60 (d, $J = 7.7$ Hz, 2H, Py), 7.89 (m, 2H, Py), 8.63 (dd, $J_a = 4.8$ Hz, 2H, Py). ^{13}C NMR (75 MHz); δ (ppm): 24.9 (2 × CH_2), 25.4 (2 × CH_2), 46.5 (2 × CH_2), 50.2 (2 × CH_2), 123.4 (CH–Py), 123.5 (CH–Py), 137.2 (CH–Py), 149.0 (CH–Py), 152.0 (C–Py). ESI-MS: *m/z* 299 ($[M+H]^+$); MS/MS, *m/z* (relative intensity): 109 (2) − $C_6H_9N_2$, 112 (5) − $C_6H_{12}N_2$, 189 (8) − $C_{12}H_{17}N_2$, 191 (100) − $C_{12}H_{19}N_2$.

N^1,N^7-Bis(2-pyridinylmethyl)-1,7-heptanediamine (BPHD): ^{1}H NMR (300 MHz); δ (ppm): 1.28 (m, 6H, 3 × CH_2), 1.71 (qui, $J = 7.5$ Hz, 4H, 2 × CH_2), 2.95 (t, $J = 7.5$ Hz, 4H, 2 × CH_2), 4.48 (s, 4H, 2 × CH_2), 7.80 (m, 2H, Py), 8.16 (d, $J = 7.9$ Hz, 2H, Py), 8.34 (m, 2H, Py), 8.82 (dd, $J_a = 5.5$ Hz, 2H, Py). ^{13}C NMR (75 MHz); δ (ppm): 25.0 (CH_2), 25.6 (2 × CH_2), 27.8 (2 × CH_2), 46.8 (2 × CH_2), 47.7 (2 × CH_2), 125.6 (CH–Py), 126.4 (CH–Py), 142.3 (CH–Py), 144.9 (CH–Py), 149.0 (C–Py). ESI-MS: *m/z* 313 ($[M+H]^+$); MS/MS, *m/z* (relative intensity): 80 (13) − C_5H_6N, 92 (18) − C_6H_6N, 109 (38) − $C_6H_9N_2$, 112 (7) − $C_7H_{14}N$, 121 (27) − $C_7H_9N_2$, 126 (31) − $C_7H_{14}N_2$, 203 (20) − $C_{13}H_{19}N_2$, 205 (100) − $C_{13}H_{21}N_2$.

N^1,N^8-Bis(2-pyridinylmethyl)-1,8-octanediamine (BPOD): ^{1}H NMR (300 MHz); δ (ppm): 1.30 (m, 8H, 4 × CH_2), 1.71 (qui, $J = 7.5$ Hz, 4H, 2 × CH_2), 2.95 (t, $J = 7.5$ Hz, 4H, 2 × CH_2), 4.44 (s, 4H, 2 × CH_2), 7.73 (t, $J = 6.5$ Hz, 2H, Py), 8.05 (d, $J = 7.9$ Hz, 2H, Py), 8.25 (m, 2H, Py), 8.79 (d, $J = 5.5$ Hz, 2H, Py). ^{13}C NMR (75 MHz); δ (ppm): 25.1 (2 × CH_2), 25.7 (2 × CH_2), 28.1 (2 × CH_2), 46.8 (2 × CH_2), 48.2 (2 × CH_2), 125.2 (CH–Py), 125.8 (CH–Py), 141.3 (CH–Py), 145.7 (CH–Py), 149.6 (C–Py). ESI-MS: *m/z* 327 ($[M+H]^+$); MS/MS, *m/z* (relative intensity): 80 (68) − C_5H_6N, 84 (11) − $C_5H_{10}N$, 92 (100) − C_6H_6N, 107 (20) − $C_6H_7N_2$, 109 (83) − $C_6H_9N_2$, 121 (23) − $C_7H_9N_2$, 126 (8) − $C_8H_{16}N$, 140 (8) − $C_8H_{16}N_2$, 217 (33) − $C_{14}H_{21}N_2$, 219 (39) − $C_{14}H_{23}N_2$.

2.3. Enzymes

Horseradish (*Armoracia rusticana*) peroxidase of specific activity 2500 nkat mg^{-1} was purchased from Sigma–Aldrich Chemie. PSAO was isolated by means of a method already published [13]. OPAO was isolated following an improved purification protocol; all steps were performed at 0–5 °C. Etiolated oat seedlings were grown as described by Smith for 14 days [14]. The seedlings (1 kg) were homogenized by a hand blender in 2 L of 0.5 M potassium phosphate buffer, pH 5.5, for 10 min. The homogenate was filtered through a nylon mesh cloth and centrifuged at 9000 × *g* for 30 min. Protamine

sulfate (5%, w/v) was added dropwise to the supernatant with constant stirring to get a final ratio of 1 g of the precipitant per 10 g of the supernatant protein. Prior to centrifugation at 9000 × *g* for 30 min, the enzyme solution was additionally stirred for 30 min. The supernatant was further fractioned by 60% saturated ammonium sulfate (390 g L^{-1}) with constant stirring and centrifuged at 9000 × *g* for 30 min. The precipitate was collected, resuspended in 40 mL of the extraction buffer and dialyzed overnight against 50 mM potassium phosphate buffer, pH 5.5, containing 0.1 M NaCl (buffer A). After centrifugation to remove precipitate, the dialyzate was loaded at a flow rate of 2 mL min^{-1} onto a DEAE-cellulose (Sigma–Aldrich Chemie) column (2.5 × 20 cm) equilibrated with buffer A. During a washing step (buffer A), the flowthrough was collected. Then it was loaded at a flow rate of 2 mL min^{-1} onto an SP-Sepharose Fast Flow (Amersham Biosciences, Uppsala, Sweden) column (2.5 × 20 cm) equilibrated with buffer A and the column was washed with the same buffer until A_{280} of the eluate decreased below 0.1. The retained proteins (visible as a yellow zone at the top of SP-Sepharose) were eluted with 50 mL of linear gradient from 0 to 100% of buffer B (0.5 M potassium phosphate buffer, pH 5.5, containing 0.5 M NaCl). Fractions containing OPAO activity (assayed with spermidine as a substrate) were collected, desalted by diafiltration with buffer A in an ultrafiltration cell equipped with a 10 kDa cut-off filter (Amicon, Danvers, MA, USA) and concentrated to a volume below 5 mL. Then two medium-pressure steps were carried out on a BioLogic Duo-Flow liquid chromatograph (Bio-Rad, Hercules, CA, USA) using the above-mentioned buffers A and B. First, the concentrated OPAO solution from SP-Sepharose purification was loaded by loop injection (500 μL) at a flow rate of 2 mL min^{-1} onto a Bio-Scale CHT5-I ceramic hydroxyapatite column (Bio-Rad) equilibrated with buffer A. The separation at a flow rate of 2 mL min^{-1} was run isocratically in the beginning (100% A, 2 min), then with successive increasing linear gradients from 0 to 70% B in 3 min and from 70 to 100% B in 8 min. An isocratic step at 100% B followed for an additional 3 min. Then a decreasing linear gradient was used from 100 to 0% B in 6 min finished by a short isocratic step (100% A) to give the total time 25 min. Fractions containing highest OPAO activity were collected, desalted and concentrated as above. Final purification was achieved on a Mono S HR 5/5 ionex column (Amersham Biosciences) equilibrated with buffer A. The concentrated enzyme solution was loaded by loop injection (500 μL) at a flow rate of 1 mL min^{-1} onto the column equilibrated with buffer A. The separation at a flow rate of 1 mL min^{-1} was run isocratically in the beginning (100% A, 2 min), then with successive increasing linear gradients from 0 to 50% B in 15 min and from 50 to 100% B in 5 min. An isocratic step at 100% B followed for an additional 3 min. Then a decreasing linear gradient was used from 100 to 0% B in 5 min finished by a short isocratic step (100% A) to give the total time 35 min. Fractions containing highest OPAO activity were collected, desalted and concentrated as above. Enzyme aliquots were stored at −80 °C.

2.4. Enzyme assays

PSAO activity was determined by spectrophotometer using a coupled reaction with horseradish peroxidase and guaiacol; putrescine served as a substrate [15]. The method was also applied for OPAO activity assay; spermidine was a substrate in this case (1 mM final concentration) [14]. Both assays were performed at 30 °C in a thermostated cell. For inhibition measurements, the reaction mixture was pipetted as follows: 1.50 mL of 0.117 M potassium phosphate buffer, pH 7.0, 25 μL of 35 mM guaiacol, 25 μL of 5 μM horseradish peroxidase (2500 nkat mg^{-1}), 10 μL of diluted enzyme and 140 μL of inhibitor (in a proper dilution to get desired concentration). The reaction was initiated by the addition of substrate (50 μL). The mixture was continually stirred and monitored by increasing absorbance at 436 nm. Inhibition constants were calculated from Lineweaver–Burk plots constructed by linear regression of the measured data (three different measurements) using the computer program Microsoft Excel 2002. Protein content was determined using the spectrophotometric method with bicinchoninic acid; BSA served as a standard [16]. Molar absorption coefficients of topaquinone at 495 nm ($\varepsilon = 4500\ M^{-1}\ cm^{-1}$) and of FAD at 450 nm ($\varepsilon = 11{,}000\ M^{-1}\ cm^{-1}$) were, respectively, used to estimate concentrations of the purified PSAO ($M_r = 145{,}000$) and OPAO ($M_r = 56{,}000$) [4,5].

2.5. MALDI-TOF mass spectrometry

One-dimensional SDS-PAGE was performed using 12% running and 4% stacking gels [17]. After electrophoresis, enzyme bands (containing 1 μg protein) were visualized by the Bio-Safe Coomassie Stain (Bio-Rad, Hercules, CA, USA). The bands were each excised from the gel slab, cut into small pieces and put into 0.65-mL microtubes. In-gel digestion was performed using 1.0 μM trypsin conjugate with raffinose [18] at 37 °C for 12 h. Peptide extraction from the digest was done according to Shevchenko et al. [19]; the extracts were dried down using a vacuum centrifuge. The recovered peptides were dissolved in 0.1% TFA (50 μL per tube). Further purification was achieved using ZipTip™ pipette tips (Millipore, Framingham, MA, USA) according to manufacturer's instructions. A saturated solution of α-cyano-4-hydroxycinnamic acid (CHCA) in 50% acetonitrile/0.1% TFA was used as a MALDI matrix. An aliquot of the purified peptides (5 μL) and 5 μL of the matrix solution were premixed in a test tube. Then 0.5 μL of the mixture was pipetted on the target plate and allowed to dry at ambient temperature. MALDI-TOF MS and MS/MS were carried out in positive ionization mode using 4700 Proteomics Analyzer MALDI-TOF/TOF mass spectrometer (Applied Biosystems, Framingham, MA, USA) equipped with a solid state laser (diode pumped Nd:YAG laser) pulsing at a repetition rate of 200 Hz (pulse duration < 500 ps) and operating at a wavelength of $\lambda = 355$ nm. Both MS and MS/MS spectra were acquired using dual-stage reflectron mirror and accumulated from up to 2500 and 20,000 shots in MS and MS/MS mode, respectively. The instrument was calibrated externally using a mixture of five peptide

Table 1
Purification of OPAO from 1 kg of 14-day-old etiolated oat seedlings

Purification step	Volume (mL)	Total activity (nkat)	Total protein (mg)	Specific activity (nkat mg^{-1})	Enrichment factor	Yield (%)
Crude extract	2200	72,000	4930	14.6	1	100
Protamine precipitation	2180	69,850	1930	36.2	2.5	97
$(NH_4)_2SO_4$ 60% sat., dialysis	142	43,890	489	89.8	6.2	60
DEAE-celullose chromatography	320	41,470	311	133.3	9.1	58
SP-Sepharose FF chromatography	45	35,280	57	618.9	42.4	49
Hydroxyapatite chromatography	15	29,800	19	1568.4	107.4	41
Mono S column chromatography	3	11,520	6.1	1888.5	129.3	16

Enzyme activity was assayed spectrophotometrically with spermidine as a substrate (see Section 2 and Ref. [14]). Protein content was estimated using bicinchoninic acid [16].

standards. Accelerating voltages applied for MS and MS/MS measurements were 20 and 8 kV, respectively. In MS/MS mode, a collision energy of 1 kV was applied and nitrogen was used as a collision gas in collision-induced dissociation experiments. Raw spectral data were further processed using DataExplorer 4.5 software (Applied Biosystems). Database searches were performed against non-redundant protein sequence databases (Swiss-Prot ver. 25.10.2005, MSDB ver. 5.7.2005, NCBInr ver. 2.11.2005) using the program Mascot ver. 1.9.05 (Matrix Science, London, UK; www.matrixscience.com).

3. Results and discussion

In this work, seven homologous *N*,*N*′-bis(2-pyridinylmethyl)diamines were synthesized and tested for possible interactions with plant amine oxidases (Fig. 1). The original idea to this project came from a study describing N^1,N^2-bis(2-pyridinylmethyl)-1,2-ethanediamine and N^1,N^3-bis(2-pyridinylmethyl)-1,3-propanediamine as manganese ligands in catalytic complexes [10]. Such ligands contain a carbon spacer between two N-donor sets. One could expect that those compounds might also form complexes with the active site copper in plant CAOs. They would also mimic binding of diamine substrates especially if there was a proper length of the spacer (ranging, for example, from 3 to 6 carbon atoms). Substrate properties with respect to CAOs were not assumed due to the lack of a primary amino group. Similar structures having even longer spacer (6–8 carbon atoms) appeared to be good candidates for substrates or inhibitors of plant PAOs. Diamines with 6–10 carbon atoms are known as powerful competitive inhibitors of maize PAO with K_i values of 10^{-7}–10^{-6} M [20]. Interestingly, *N*,*N*′-bis(benzyl)polyamine analogs derived by binding benzylaminopropyl groups to nitrogens of C4–C10 diamines have already been described as substrates for a mammalian PAO [21]. Their enzymatic conversion was dependent on molecular O_2 and resulted in debenzylation and the release of polyamine analogs with free terminal primary amino groups. We were therefore interested whether *N*,*N*′-bis(2-pyridinylmethyl)diamines might behave as common inhibitors of

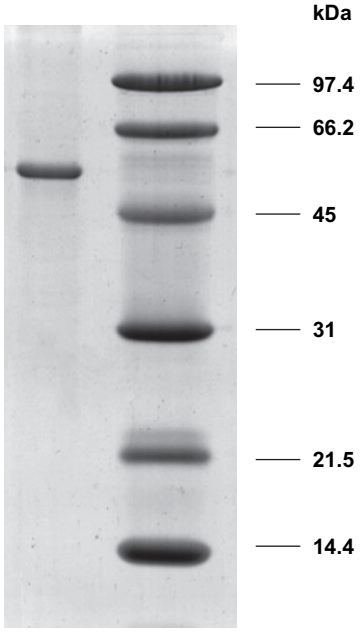

Fig. 2. SDS-PAGE of purified OPAO. From the left, OPAO sample (2 μg) and low-range protein standards (Bio-Rad) with the indicated molecular mass. Proteins were visualized by the Bio-Safe Coomassie Stain (Bio-Rad).

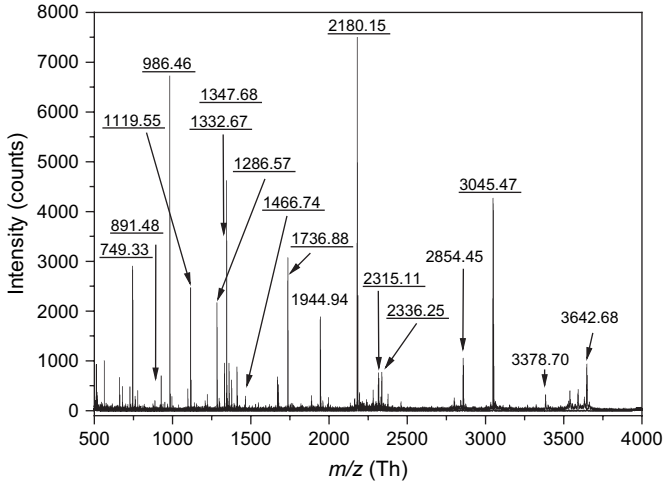

Fig. 3. MALDI-TOF peptide mass fingerprinting of OPAO. A sample of the enzyme was resolved by SDS-PAGE and then subjected to in-gel digestion by modified bovine trypsin [18]. MALDI probe was prepared using a dried droplet method with CHCA matrix. Then MALDI-TOF mass spectra were acquired in positive ionization mode. Peaks with the underlined *m*/*z* values (rounded to two decimal places) represent peptides, which were further subjected to de novo sequencing (see Table 2 and Fig. 4).

CAOs and PAOs despite the different molecular structures and catalytic mechanisms of the enzymes.

Kinetic measurements were performed with PSAO and OPAO as typical representatives of both types of amine oxidases. Whereas PSAO was obtained by a routine purification, OPAO was isolated using a new method, which omitted the usually involved acetone powder extraction [5]. The final PSAO preparation had a specific activity of 720 nkat mg^{-1}, enrichment factor was 80 and yield 38%. For OPAO, the purification characteristics were as follows: specific activity 1890 nkat mg^{-1}, enrichment factor 129 and yield 16% (Table 1). SDS-PAGE confirmed homogeneity of the purified OPAO by a single protein band referring to a molecular mass of 56 kDa (Fig. 2). Compared to a previously published protocol, which involves the acetone powder extraction and three chromatographic steps [22], we achieved much higher specific activity (by 60%) at a similar yield per 1 kg of the starting material. An additional improvement resides in facilitating the seedling extraction. Preparation of acetone powder requires careful experimental work unless it brings a risk of enzyme denaturation.

A MALDI-TOF peptide mass fingerprint of OPAO is shown in Fig. 3, which was acquired after in-gel digestion by modified trypsin [18]. Database searches of the respective peaklist were performed using the program Mascot. Interestingly, the fingerprint was assigned in the following order to barley polyamine oxidase-isoform 1 (BPAO1) and maize polyamine oxidase (MPAO) in the Swiss-Prot, MSDB and NCBInr protein sequence databases despite relatively low probability-based score values (50–60). The retrieved accession numbers were Q93WM8 (BPAO1) and Q9FXZ9 (MPAO) in the Swiss-Prot and MSDB databases. The corresponding accession numbers in the NCBInr database were CAC42118 (BPAO1) and CAC04002 (MPAO). It should be noted here that OPAO sequence is not yet available in the mentioned databases. Prior to de novo sequencing, this clearly indicated a large homology of OPAO to other plant PAOs. In order to obtain basic

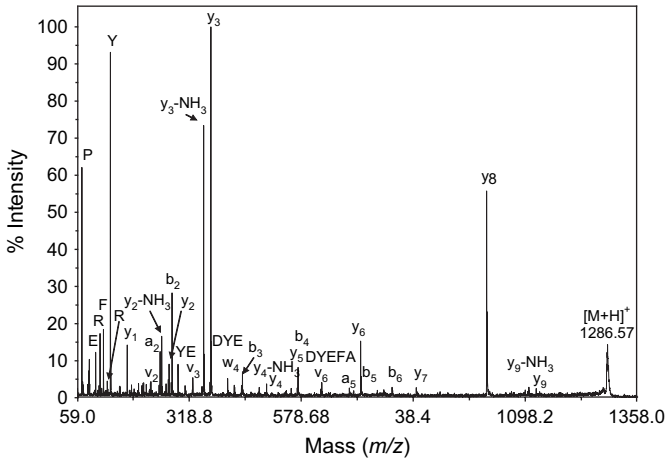

Fig. 4. Example of de novo peptide sequencing of OPAO. A tryptic peptide from OPAO was submitted to a tandem mass spectrometry analysis using MALDI-TOF/TOF instrument. Precursor ion with *m/z* 1286.57 was subjected to collision-induced dissociation using nitrogen as a collision gas. Fragment ions yielding a sequence YDYEFAEPPR of the analyzed peptide are appropriately labeled.

structural informations with respect to OPAO, de novo peptide sequencing was performed using the collision-induced dissociation on MALDI-TOF/TOF instrument. The MS/MS analyses resulted in 13 peptide sequences (Table 2) giving a total of 141 amino acids. Raw spectral data of the sequenced peptides are available from the authors upon request. Fig. 4 shows an example of the acquired MS/MS spectra: a tryptic peptide with *m/z* 1286.57 selected from the MS spectrum (see also Fig. 3) was analyzed yielding a sequence YDYEFAEPPR. Using the program CLUSTAL W [23], we obtained a multiple sequence alignment of the analyzed peptides and the whole amino acid sequences of MPAO, BPAO1 and BPAO2 (Fig. 5). The alignment clearly demonstrates that OPAO is largely homologous to plant PAOs, namely two, BPAO1 and MPAO. As can be deduced from the alignment, three of the sequenced OPAO

Table 2
De novo sequencing of OPAO tryptic peptides

No.	Sequence	Observed mass (Da)	Calculated mass (Da)[a]	Delta (Da)	Missed cleavages
1	WWSDR	749.3320	749.3365	−0.0045	0
2	KFWPEGK	891.4820	891.4723	0.0097	1
3	YEYDQLR[c]	986.4617	986.4578	0.0039	0
4	EFFLYASSR[c]	1119.5532	1119.5469	0.0063	0
5	YDYEFAEPPR	1286.5745	1286.5688	0.0057	0
6	GREFFLYASSR[c]	1332.6722	1332.6695	0.0027	1
7	GTFSNWPIGVNR[b]	1347.6849	1347.6810	0.0039	0
8	YEYDQLRAPVGR[c]	1466.7413	1466.7385	0.0028	1
9	GYEAVVYYLAGQYLK[c]	1736.8794	1736.8894	−0.0100	0
10	LSEAGITDLVILEATDHIGGR[c]	2180.1453	2180.1557	−0.0104	0
11	GTFSNWPIGVNRYEYDQLR[c]	2315.1091	2315.1204	0.0113	1
12	RLSEAGITDLVILEATDHIGGR[c]	2336.2473	2336.2568	−0.0095	1
13	VTSLQNVVPLATFEDFGDDVYFVADQR[c]	3045.4734	3045.4839	−0.0105	0

The peptides were individually selected from peptide mass fingerprint of OPAO (see Fig. 3) and then subjected to the collision-induced dissociation by nitrogen gas on 4700 Proteomics Analyzer MALDI-TOF/TOF mass spectrometer. The MS/MS data were processed using DataExplorer 4.5 software.

[a] Monoisotopic mass $[M + H]^+$.

[b] Isoleucine confirmed by a fragment ion with *m/z* 513.3349 (w-ion) − this refers also to peptide no. 11.

[c] Leucines and isoleucines deduced from the homology with BPAO1 and MPAO (Fig. 5).

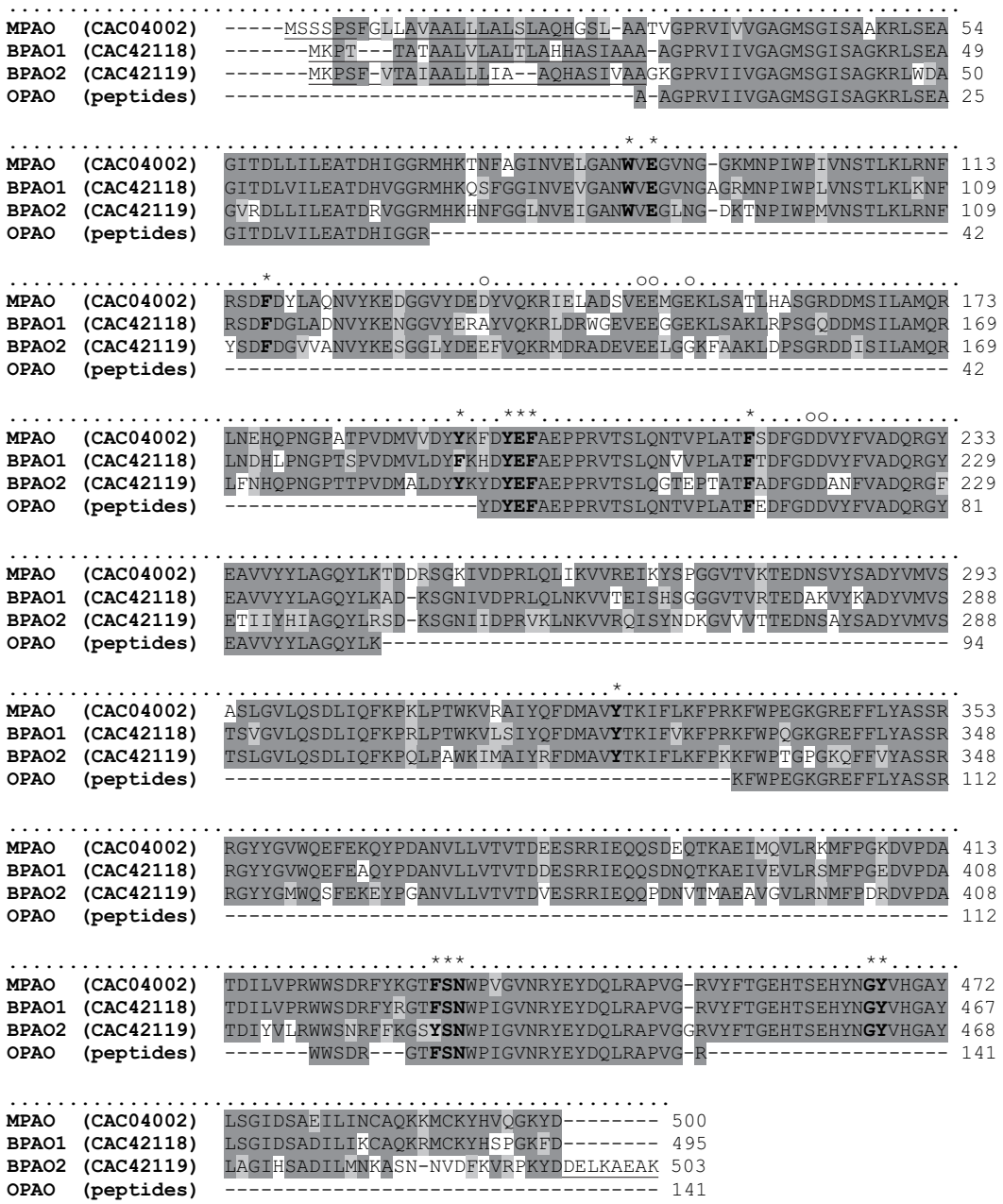

Fig. 5. Amino acid sequence comparison of plant PAOs. Multiple sequence alignment was performed by the program CLUSTAL W [23]; graphic view was obtained using BioEdit v. 7.0.1. software (Isis Pharmaceuticals, Inc.). The abbreviations MPAO, BPAO1, BPAO2 and OPAO refer to the enzymes from maize, barley (isoforms 1 and 2) and oat, respectively. Gray boxes indicate identical residues (dark gray) or similar residues (light gray). Signal peptide sequences are in bold underlined letters; those residues putatively involved in the catalytic activity are in bold and indicated by asterisk, and those composing the tunnel entrance are labeled by circle (○) [24]. Codes in parentheses represent the respective protein accession numbers in the NCBInr protein sequence database. The N-terminal amino acid sequence (AAGPRVIIVGAGMSGISAGKR) of OPAO was previously analyzed by Edman degradation [5].

peptides comprise catalytic residues of the tunnel-shaped active site of plant PAOs (nos. 5, 7 and 13 in Table 2). One of these peptides (no. 13) additionally contains two aspartic acid residues from the tunnel entrance [24]. The other peptides were aligned in a distribution partially covering all sequence regions of plant PAOs (Fig. 5).

None of the synthesized *N*,*N*′-bis(2-pyridinylmethyl)diamines was found to be a substrate of the enzymes since no oxidative conversion (i.e. hydrogen peroxide production) was detected by the guaiacol spectrophotometric method. For that reason the compounds were tested as enzyme inhibitors: they were added to PSAO and OPAO samples in 0.1 M potassium phosphate buffer, pH 7.0 and the reaction mixtures were assayed for enzyme activity. Fast inhibitions occurred as no time lag in their development was observed. This was analyzed by preincubation of the enzymes with the inhibitors prior to the activity assay (5, 10 and 15 min). Reversibility of the inhibitions was verified by dialysis of the reaction

mixtures and subsequent activity assay. Inhibition constants were calculated from data sets measured using varying substrate concentrations for each fixed inhibitor concentration. PSAO reaction with the substrate putrescine was inhibited competitively by all studied compounds (Table 3). As regards to OPAO, the inhibitions were also competitive with the exception of BPED, which showed a non-competitive inhibition towards the substrate spermidine (Table 3). PSAO was inhibited with K_i values of 10^{-4} M (only BPOD provided a K_i value of 10^{-5} M). The potency of OPAO inhibition increased continually with the increasing number of methylene groups in the inhibitor structure and it spanned two orders of magnitude within the tested compounds (Table 3). The biggest difference was observed between the K_i values determined for BPED (4×10^{-3} M) and for BPOD (2×10^{-5} M). Figs. 6 and 7 demonstrate some illustrative double reciprocal plots of the measured inhibition data.

The active site existing in each of the two PSAO subunits is deeply buried and therefore not exposed to the bulk solvent. The highly flexible topaquinone cofactor is accessible through a narrow channel whose entrance is opened upon structural rearrangement [6]. PSAO shows a wide specificity towards diamines of various lengths [25]. Relative rates of oxidation of cadaverine, 1,6-hexanediamine, 1,7-heptanediamine and 1,8-octanediamine at a saturation concentration (2.5 mM) measured in this work were 110, 31, 20 and 11%, respectively, when that of putrescine oxidation was taken as 100%. K_m values were all of 10^{-4} M. Crystallographic data on substrate binding to PSAO are not yet available (www.rcsb.org), however, it is clear that electrostatic and hydrophobic forces mediate substrate docking like in other CAOs [26,27]. It is known that substrate binding is enabled by conformational changes at the surface of PSAO molecule [6]. The studied *N*,*N*′-bis(2-pyridinylmethyl)diamines function as competitive inhibitors of PSAO and thus they should bind at the active site. Hydrophobic interactions seem to play an important role in this process as BPOD (having the longest aliphatic core chain) provided the lowest K_i value. However, the binding is rather weak. Inhibitor concentrations, which are necessary for significant competition with the substrate putrescine, are comparable with its K_m value. Copper complexing is not expected because Cu(II)-chelators usually provide a strong non-competitive inhibition [28].

Table 3
Inhibition constants determined for inhibitions of PSAO and OPAO by *N*,*N*′-(2-pyridinylmethyl)-diamines

Compound	PSAO		OPAO	
	K_i (mM)	Inhibition type	K_i (mM)	Inhibition type
BPED	0.10	C	3.62	NC
BPRD	0.20	C	2.16	C
BPBD	0.11	C	1.43	C
BPPD	0.22	C	0.30	C
BPXD	0.25	C	0.11	C
BPHD	0.10	C	0.08	C
BPOD	0.07	C	0.02	C

C, competitive inhibition; NC, non-competitive inhibition.

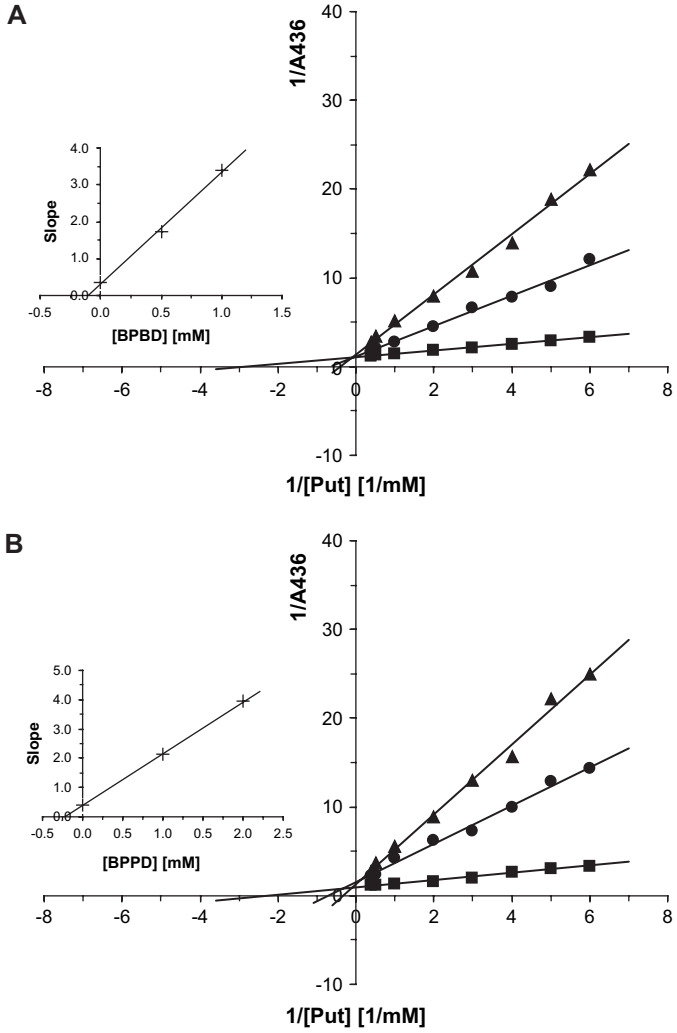

Fig. 6. Double reciprocal plots of competitive inhibitions of PSAO by *N*,*N*′-bis(2-pyridinylmethyl)diamines with putrescine (Put) as substrate. Initial rates were determined by the guaiacol spectrophotometric method. The assay was carried out in 0.1 M potassium phosphate buffer, pH 7.0, at 30 °C. (A) BPBD, final concentrations: ■, 0 mM; ●, 0.5 mM; and ▲, 1.0 mM, $K_i = 0.11$ mM. (B) BPPD, final concentrations: ■, 0 mM; ●, 1 mM; and ▲, 2 mM, $K_i = 0.22$ mM. The corresponding insets show secondary plots of slopes against the inhibitor concentration.

OPAO and MPAO show very similar substrate preference with respect to spermine and spermidine oxidation; both enzymes also oxidize acetylpolyamines [5]. As can be seen in the crystal structure of MPAO (www.rcsb.org; PDB accession number 1B37), the active site consists of a ''U-shaped'' tunnel, which passes through the protein molecule [7]. There is a hydrophobic pocket at the wider catalytic tunnel opening, whereas the other arm presents mostly oxygen atoms on its surface. The bending point of the tunnel comprises a pair of Glu side chains in front of the cofactor flavin ring and it is flanked by some aromatic residues [7]. For the homologous OPAO (Fig. 5) we may anticipate a very similar active site configuration. The studied *N*,*N*′-(2-pyridinylmethyl)diamines are characterized by the presence of terminal aromatic rings, which seem to fit the hydrophobic pocket of OPAO. The correct placement of the inhibitors could be further facilitated by

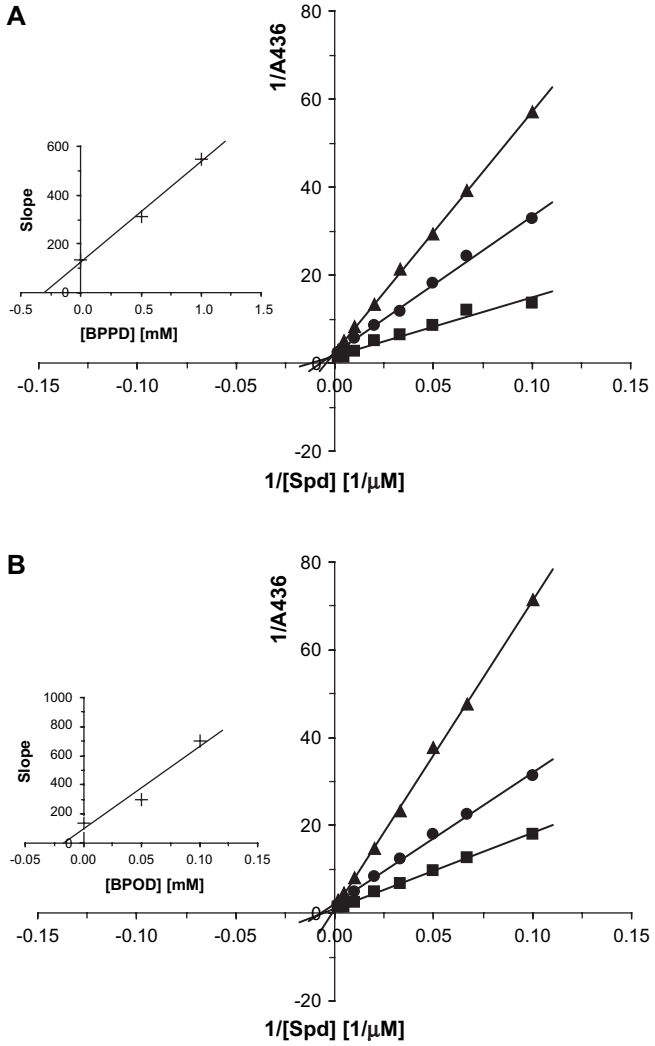

Fig. 7. Double reciprocal plots of competitive inhibitions of OPAO by *N*,*N*′-bis(2-pyridinylmethyl)diamines with spermidine (Spd) as substrate. Initial rates were determined by the guaiacol spectrophotometric method. The assay was carried out in 0.1 M potassium phosphate buffer, pH 7.0, at 30 °C. (A) BPPD, final concentrations: ■, 0 mM; ●, 0.5 mM; and ▲, 1.0 mM, $K_i = 0.30$ mM. (B) BPOD, final concentrations: ■, 0 mM; ●, 0.05 mM; and ▲, 0.10 mM, $K_i = 0.02$ mM. The corresponding insets show secondary plots of slopes against the inhibitor concentration.

contacts between their alkyl spacer chains and aromatic residues of the tunnel plus a polar interaction of the secondary amino groups [7]. This would explain the gradually increasing inhibition effect of the compounds as a function of the number of methylene groups in their molecules. The shortest compound BPED probably does not bind at the active site. It might stay by the hydrophobic entrance and therefore produce weak non-competitive inhibition.

Numerous aromatic substituted diamines including BPBD were previously characterized for their cytotoxicity against human breast and prostate tumor cell lines [12]. Such compounds were generally intended to disturb polyamine metabolism. Whereas the most potent compounds demonstrated effects at micromolar concentrations, BPBD itself showed an unfavorably high IC_{50} value of 10^{-3} M [12]. Interestingly, bis(benzyl)polyamine analogs show remarkable antiparasitic effects [20]. An antitumor activity of several unsubstituted benzyldiamines such as dibenzylputrescine has been reported [29]. In this context, we conclude that some of the studied *N*,*N*′-bis(2-pyridinylmethyl)diamines (namely the C7 and C8 diamine analogs, which demonstrated lowest K_i values in this study) might have a potential to be starting structures in design of future multifunctional compounds with a potential in the modulation of polyamine levels via the inhibition of diamine and polyamine oxidases. We believe that introducing a proper chemical substitution at the pyridine rings of the pyridinyldiamines might increase inhibition properties of the compounds towards the enzymes. This might also positively influence their biological activity in the sense of a potential use as cytotoxic agents. For example, Burns et al. observed a large influence of both chemical nature and positioning of substituents at the aromatic rings of bis(benzyl)-1,4-butanediamine on IC_{50} values in tests on cytotoxicity [12].

Acknowledgments

The authors gratefully acknowledge financial help of the grant MSM 6198959216 from the Ministry of Education, Youth and Sports, Czech Republic (MSMT). Pavel Peč was supported by another grant (MSM 6198959215) from the same provider.

References

[1] A. Bouchereau, A. Aziz, F. Larher, J. Martin-Tanguy, Polyamines and environmental challenges: recent development, Plant Sci. 140 (1999) 103–125.
[2] A. Cona, G. Rea, R. Angelini, R. Federico, P. Tavladoraki, Functions of amine oxidases in plant development and defence, Trends Plant Sci. 11 (2006) 80–88.
[3] I. Frébort, O. Adachi, Copper/quinone-containing amine oxidases, an exciting class of ubiquitous enzymes, J. Ferment. Bioeng. 80 (1995) 625–632.
[4] R. Medda, A. Padiglia, G. Floris, Plant copper-amine oxidases, Phytochemistry 39 (1995) 1–9.
[5] M. Šebela, A. Radová, R. Angelini, P. Tavladoraki, I. Frébort, P. Peč, FAD-containing polyamine oxidases: a timely challenge for researchers in biochemistry and physiology of plants, Plant Sci. 160 (2001) 197–207.
[6] V. Kumar, D.M. Dooley, H.C. Freeman, J.M. Guss, I. Harvey, M.A. McGuirl, M.C.J. Wilce, V.M. Zubak, Crystal structure of a eukaryotic (pea seedling) copper-containing amine oxidase at 2.2 Å resolution, Structure 4 (1996) 943–955.
[7] C. Binda, A. Coda, R. Angelini, R. Federico, P. Ascenzi, A. Mattevi, A 30 Å long U-shaped catalytic tunnel in the crystal structure of polyamine oxidase, Structure 7 (1999) 265–276.
[8] A. Padiglia, R. Medda, J.Z. Pedersen, A. Lorrai, P. Peč, I. Frébort, G. Floris, Inhibitors of plant copper amine oxidases, J. Enzym. Inhib. 13 (1998) 311–325.
[9] C. Binda, R. Angelini, R. Federico, P. Ascenzi, A. Mattevi, Structural bases for inhibitor binding and catalysis in polyamine oxidase, Biochemistry 40 (2001) 2766–2776.
[10] J. Brinksma, Manganese catalysts in homogeneous oxidation reactions, PhD thesis, University of Groningen, 2002.
[11] A. Sánchez-Sandoval, C. Álvarez-Toledano, R. Gutiérrez-Pérez, Y. Reyes-Ortega, A modified procedure for the preparation of linear polyamines, Synth. Commun. 33 (2003) 481–492.
[12] M.R. Burns, S. LaTurner, J. Ziemer, M. McVean, B. Devens, C.L. Carlson, G.F. Graminski, S.M. Vanderwerf, R.S. Weeks,

J. Carreon, Induction of apoptosis by aryl-substituted diamines: role of aromatic group substituents and distance between nitrogens, Bioorg. Med. Chem. Lett. 12 (2002) 1263–1267.

[13] M. Šebela, L. Luhová, I. Frébort, H.G. Faulhammer, S. Hirota, L. Zajoncová, V. Stužka, P. Peč, Analysis of the active sites of copper/topa quinone-containing amine oxidases from *Lathyrus odoratus* and *L. sativus* seedlings, Phytochem. Anal. 9 (1998) 211–222.

[14] T.A. Smith, Polyamine oxidase (oat seedlings), Methods Enzymol. 94 (1983) 311–314.

[15] I. Frébort, A. Haviger, P. Peč, Employment of guaiacol for the determination of activities of enzymes generating hydrogen peroxide and for the determination of glucose in blood and urine, Biológia (Bratislava) 44 (1989) 729–737.

[16] P.K. Smith, R.I. Krohn, G.T. Hermanson, A.K. Mallia, F.H. Gartner, M.D. Provenzano, E.K. Fujimoto, N.M. Goeke, B.J. Olson, D.C. Klenk, Measurement of protein using bicinchoninic acid, Anal. Biochem. 150 (1985) 76–85.

[17] U.K. Laemmli, Cleavage of structural proteins during the assembly of the head of bacteriophage T4, Nature 227 (1970) 650–685.

[18] M. Šebela, T. Štosová, J. Havliš, N. Wielsch, H. Thomas, Z. Zdráhal, A. Shevchenko, Thermostable trypsin conjugates for high throughput proteomics: synthesis and performance evaluation, Proteomics 6 (2006) 2959–2963.

[19] A. Shevchenko, I. Chernushevich, M. Wilm, M. Mann, De novo peptide sequencing by nanoelectrospray tandem mass spectrometry using triple quadrupole and quadrupole/time-of-flight instruments, Methods Mol. Biol. 146 (2000) 1–16.

[20] A. Cona, F. Manetti, R. Leone, F. Corelli, P. Tavladoraki, F. Polticelli, M. Botta, Molecular basis for the binding of competitive inhibitors of maize polyamine oxidase, Biochemistry 43 (2004) 3426–3435.

[21] A.J. Bitonti, J.A. Dumont, T.L. Bush, D.M. Stemerick, M.L. Edwards, P.P. McCann, Bis(benzyl)polyamine analogs as novel substrates for polyamine oxidase, J. Biol. Chem. 265 (1990) 382–388.

[22] R. Federico, C. Alisi, F. Forlani, R. Angelini, Purification and characterization of oat polyamine oxidase, Phytochemistry 28 (1989) 2045–2046.

[23] J.D. Thompson, D.G. Higgins, T.J. Gibson, CLUSTAL W: improving the sensitivity of progressive multiple sequence alignment through sequence weighting, position-specific gap penalties and weight matrix choice, Nucleic Acids Res. 22 (1994) 4673–4680.

[24] M. Cervelli, A. Cona, R. Angelini, F. Polticelli, R. Federico, P. Mariottini, A barley polyamine oxidase isoform with distinct structural features and subcellular localization, Eur. J. Biochem. 268 (2001) 3816–3830.

[25] J.M. Hill, P.J.G. Mann, Further properties of the diamine oxidase of pea seedlings, Biochem. J. 91 (1964) 171–182.

[26] M. Lunelli, M.L. Di Paolo, M. Biadene, V. Calderone, R. Battistutta, M. Scarpa, A. Rigo, G. Zanotti, Crystal structure of amine oxidase from bovine serum, J. Mol. Biol. 346 (2005) 991–1004.

[27] A.P. Duff, A.E. Cohen, P.J. Ellis, J.A. Kuchar, D.B. Langley, E.M. Shepard, D.M. Dooley, H.C. Freeman, J.M. Guss, The crystal structure of *Pichia pastoris* lysyl oxidase, Biochemistry 42 (2003) 15148–15157.

[28] K. Mlíčková, M. Šebela, R. Cibulka, I. Frébort, P. Peč, F. Liška, K. Tanizawa, Inhibition of copper amine oxidases by pyridine-derived aldoximes and ketoximes, Biochimie 83 (2001) 995–1002.

[29] G. Aizencang, P. Harari, G. Buldain, L. Guerra, M. Pickart, P. Hernandez, B. Frydman, Antiproliferative effects of N^1,N^4-dibenzylputrescine in human and rodent tumor cells, Cell. Mol. Biol. 44 (1998) 615–625.